Experiment E092 - Franck-Hertz Collision Experiment

Robin Hoffmann*, Arik Bürkle†, Valentin Ertl‡

June 10, 2025

Kurzfassung

This report discusses the Franck-Hertz experiment, which can be used to validate the Bohr atomic model by observing the first excited energy level of neon gas using a tetrode. With the collected data from our experiment, this energy level is determined to be $E_a = 16{,}3(9)\,\mathrm{eV}$ in the course of this report.

*robin.hoffmann@student.uibk.ac.at
†arik.buerkle@Student.uibk.ac.at
‡valentin.ertl@student.uibk.ac.at

Contents

1 Introduction

The Franck-Hertz experiment, conducted in 1914 by James Franck and Gustav Hertz, represents a landmark in the field of quantum physics. This experiment provided the first direct evidence for the quantized nature of energy levels within atoms, a cornerstone of modern atomic theory. By examining the behavior of electrons as they interact with mercury atoms, Franck and Hertz were able to validate the predictions made by Niels Bohr regarding the discrete energy levels of electrons in an atom. The experimental setup consists of an evacuated tube filled with mercury vapor, wherein electrons are emitted from a heated cathode and accelerated through a known potential difference towards a positively charged grid. Beyond this grid lies a collecting plate. As the electrons traverse the tube, they collide with mercury atoms. By varying the accelerating voltage, Franck and Hertz observed the current reaching the collecting plate. They noted distinct drops in current at specific voltages, corresponding to the energy required to excite the mercury atoms from their ground state to higher energy levels. This phenomenon can be explained by the quantum theory of energy absorption. When an electron possesses just the right amount of kinetic energy, it can transfer this energy to a mercury atom in a perfectly elastic collision, exciting the atom to a higher energy state. Consequently, the electron loses a significant portion of its kinetic energy, resulting in a noticeable drop in the measured current. These distinct energy absorption points underscore the quantized nature of atomic energy levels, as the electrons must impart specific quantities of energy to the mercury atoms. The Franck-Hertz experiment not only reinforced the quantization concept but also provided a practical method to measure the energy levels of atoms. The discrete energy values obtained from the experiment were in remarkable agreement with Bohr's theoretical predictions, thereby cementing the Bohr model of the atom and advancing the development of quantum mechanics. This experiment exemplifies the transition from classical to quantum physics, illustrating the necessity of a new paradigm to understand atomic and subatomic phenomena. The aim of our experiment is to imitate this experiment, just as James Franck and Gustav Hertz did in 1914, and thus prove the quantization of energy levels.

2 Theory

2.1 The Bohr Atomic Model

The Bohr atomic model is characterized by the quantized energy levels of the electrons orbiting the nucleus. In this model, electrons can only occupy fixed discrete energy levels E_n, where n is a natural number. Additionally, the atom can only absorb or release energy that corresponds to an energy quantum. The energy of the light emitted by such an atom can therefore be described by

$$\Delta E = \frac{hc}{\lambda} \tag{1}$$

where h is Planck's constant, λ is the wavelength of the emitted light, and c is the speed of light. This process is called spectroscopy and can be used to study atoms and their energy levels.

2.2 Inelastic Collisions

In our experiment, we will use a different method than light to determine the energy levels of an atom. By sending electrons through neon gas in a tetrode (Figure 1), we create an environment where collisions between electrons from the tetrode and gas atoms can occur. If the electrons do not have enough energy to excite the atom, the collision is elastic; otherwise, the collision is inelastic, and the electron transfers a discrete amount of energy to the atom, causing it to become excited. The first excited state E_a of the atom corresponds to the energy the electron lost, which can be observed by a drop in the anode current.

$$e \cdot \Delta U_B = E_a \tag{2}$$

where ΔU_B is the distance between two minima in the collected anode current and e is the elementary charge of an electron. This can be further related to the mean free path length λ and the acceleration section of the tetrode as follows:

$$\Delta U_B(n) = U_{B,n} - U_{B,n-1} = \frac{E_a}{e} \cdot \left[1 + \frac{\lambda}{L} \cdot (2n-1)\right] \tag{3}$$

where n is the index of the minima.

2.3 Mean Free Path Length

The mean free path length describes the average distance an electron can travel before colliding with a gas atom after reaching the specific energy to potentially excite an atom. This is a statistical process that influences the distance between the minima of the collected anode current.

$$\lambda = \frac{eL}{2E_a} \cdot \frac{d}{dn} \Delta U_B(n) \tag{4}$$

3 Experiment setup and execution

In this experiment we need following components:

- Franck-Hertz tube
- Oscilloscope
- Operating device of the Franck-Hertz tube with built-in current amplifier
- Various connection cables

The Franck-Hertz tube used in this experiment corresponds to a tetrode with an indirectly heated barium oxide cathode, a grid-shaped control electrode, a grid-shaped anode, and a collecting electrode. The tube has a hole through which a glow can be observed. This glow is produced by the relaxation of an electron, which subsequently emits a photon with a specific wavelength. By applying a heating voltage to the cathode, electrons are emitted from it and accelerated towards the collecting electrode by an accelerating voltage. By applying a counter-voltage to the electrode between the anode and the collecting electrode, it is ensured that electrons that have inelastically interacted with neon atoms do not reach the collecting electrode. This results in the characteristic minima in the current-voltage curve of the Franck-Hertz tube becoming visible. The circuit diagram of the experimental setup and the Franck-Hertz tube used are shown in Figure 1.

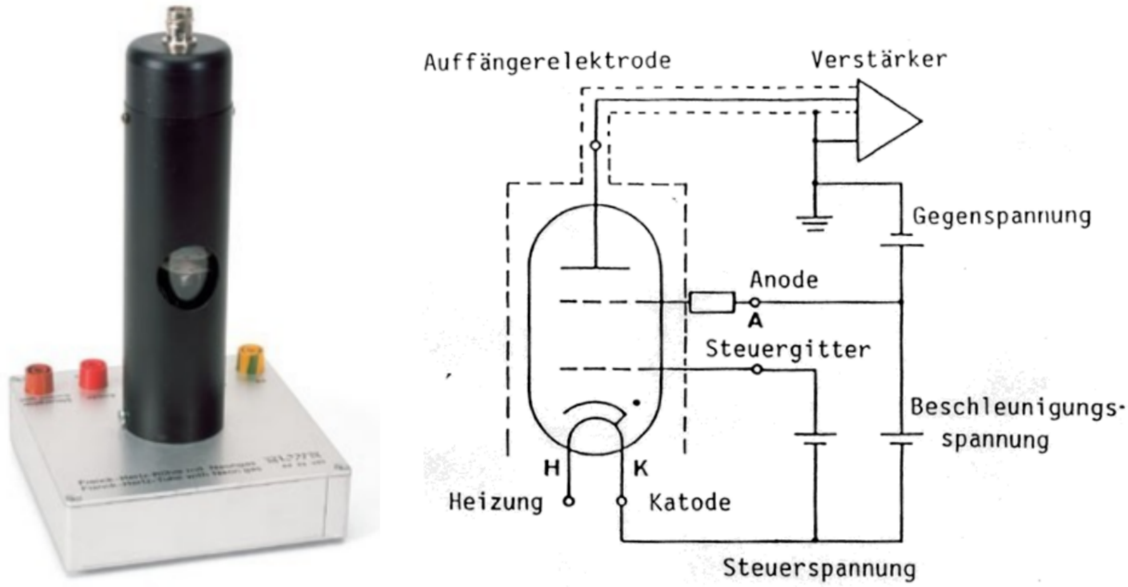

Figure 1: Franck-Hertz tube used in the experiment (left) and experimental circuit (right). Taken from [1]

Figure 2 shows the experimental setup as it was set up in the practical room. Figure 3 shows a sketch of the experimental setup.
The various voltages, such as the heating voltage or the accelerating voltage, can be varied on the operating device of the Franck-Hertz tube, which has a built-in current amplifier. The characteristic curve is measured on the oscilloscope, which is connected to the output of the accelerating voltage and the output of the Franck-Hertz tube. The accelerating voltage used is a so-called sawtooth voltage. By varying the different values for the diffrent applied voltages (heating voltage, control voltage, accelerating voltage, and counter-voltage), different characteristic curves

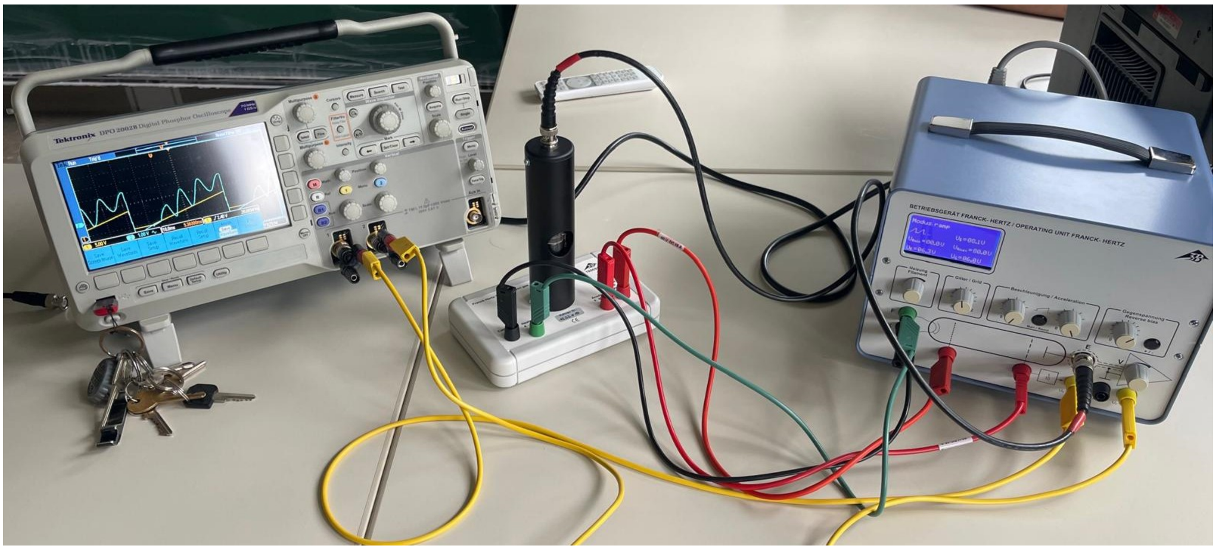

Figure 2: Experimental setup. In the middle, the Franck-Hertz tube used is visible. On the right is the operating device for the Franck-Hertz tube with the built-in current amplifier. On the left is an oscilloscope, where the characteristic curve can be read and measured.

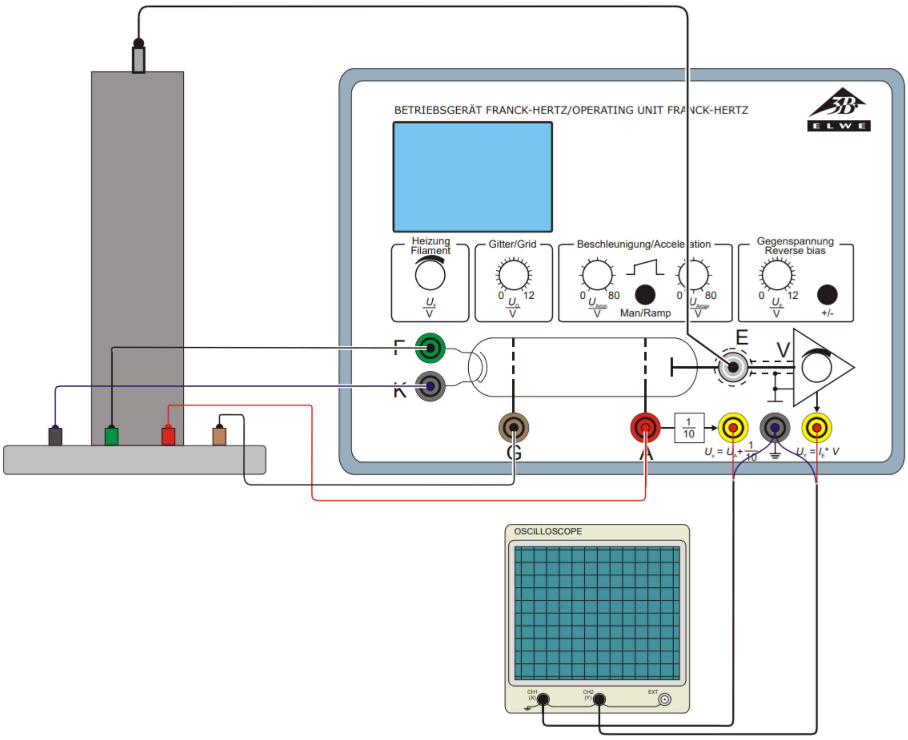

Figure 3: Sketch of the experimental setup. Taken from [2]

are measured. First we collect the anode current vs U_2 for at least five different values of U_1. Second we collect the anode current vs U_2 for at least five different values of U_3. And at the end we collect one data set of averaged anode current vs U_2 with fixed U_1 and U_3, which is the basis of our analysis. The heating voltage is adjusted so that a glow is visible in the opening of the tube.

4 Experimental results

In the first part of the experiment, the control grid voltage U_1 was varied from 6V to 10V. The trend is shown in Figure 4. The characteristic minima, caused by atomic excitation, are evident. However, we will not focus on atomic excitation just yet, but rather on the effects of the control grid voltage. It can be observed that a higher control grid voltage results in a larger current I reaching the anode. This is due to the fact that higher control grid voltages release more electrons from the cathode. In Figure 5, a linear fit was applied to each dataset. It is clearly visible that the slope of the data increases with higher control grid voltage U_1.

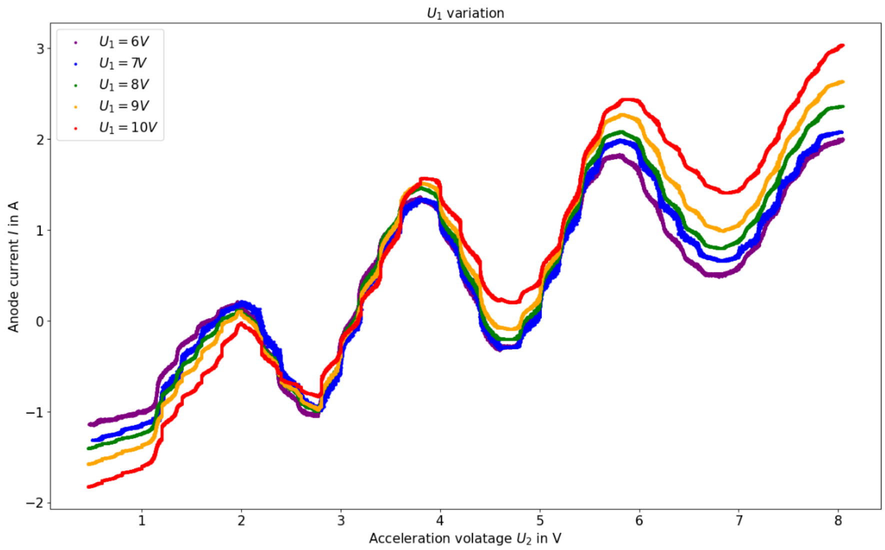

Figure 4: The figure plots the anode current I against the acceleration voltage U_2. The data for different measurements with varying control grid voltage U_1 from 6V to 10V are depicted in different colors (see legend).

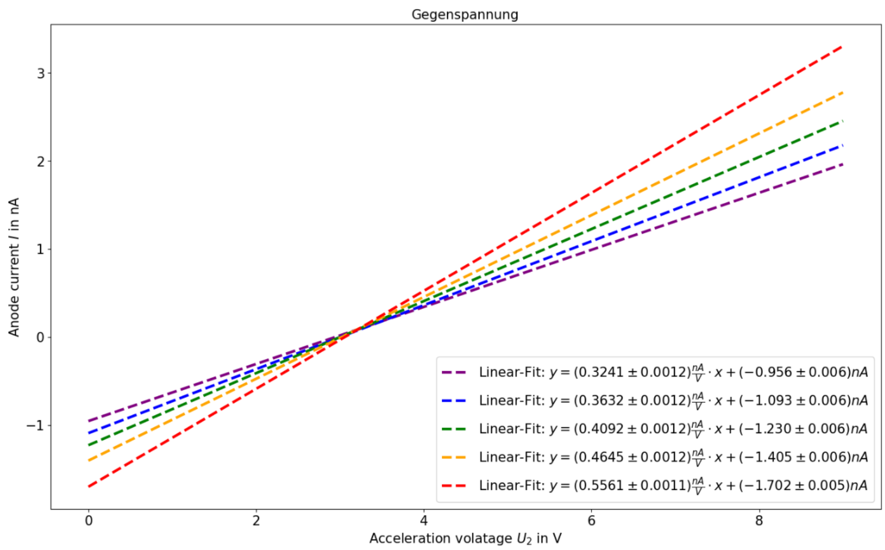

Figure 5: The figure displays the linear fits of the data from Figure 4, with the equations of the linear fits provided in the legend.

In the second part of the experiment, the reverse bias voltage U_3 was varied from 6V to 10V. The trend is shown in Figure 6. It is clearly observable that at higher reverse bias voltage, a lower current is measured at the anode. This is because electrons with insufficient energy are filtered out by the final grid.

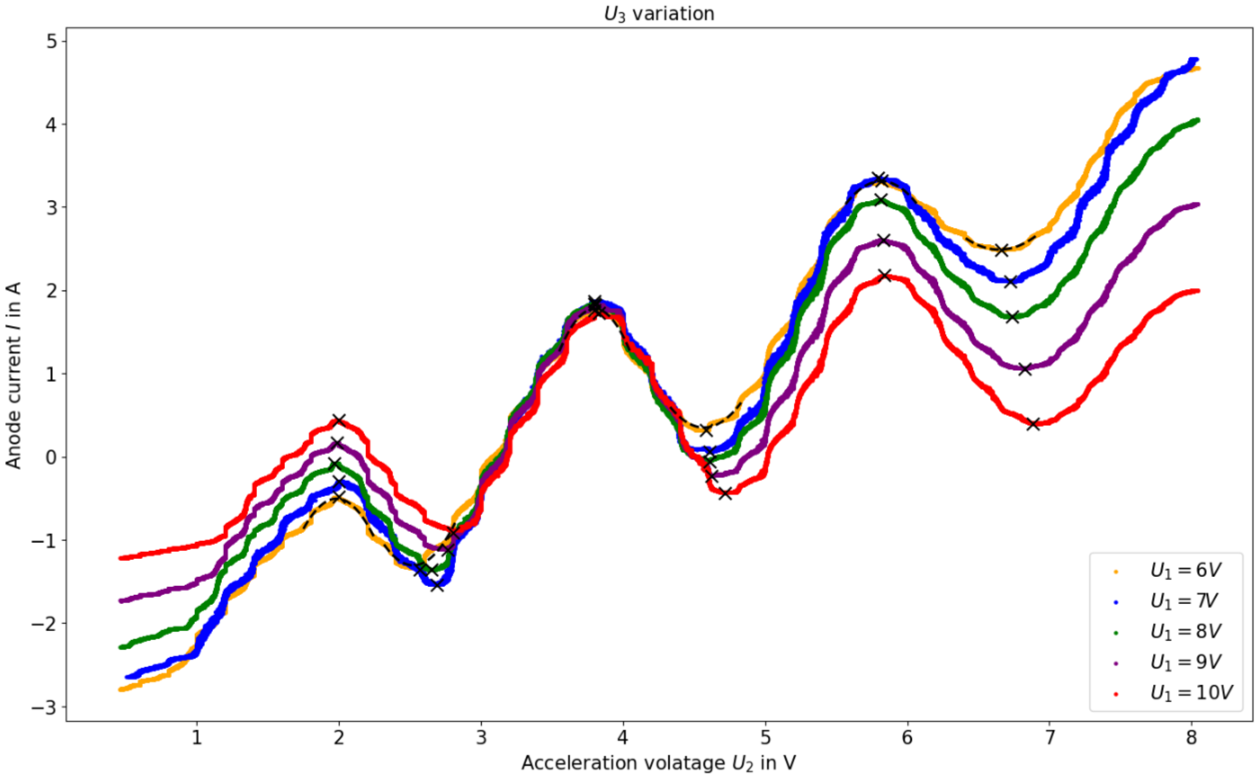

Figure 6: The figure plots the anode current I against the acceleration voltage U_2. The data for different measurements with varying reverse bias voltage U_3 from 6V to 10V are depicted in different colors (see legend). The extrema are marked with black crosses, and for each extremum of the orange curve, a parabolic fit in vertex form has been applied, indicated by the dashed black line.

Using this plot, the excitation energy of the first excited state E_a of neon gas is to be calculated. For this, the distance between adjacent minima or maxima can be measured and related to the excitation energy as described in Equation 2. The extrema of the functions were determined using the Python function "find-peaks" and are presented in Table 1. Since the function does not account for errors, a parabolic function in vertex form was fitted to each peak of the orange function to constrain the error. The parameters of the various fit functions are shown in Table 1. It was found that the extrema of the parabolic function were less accurate, so ultimately the extrema from the "find-peaks" function were used, but the error for the x-deviation (in this case the variable d) was applied to account for the extrema with errors (see Table 1).

Errors were only considered for the orange function as the fitting routine encountered issues. However, the curves of the extrema are very similar and thus comparable. It will become apparent later that the error in the x-value of the extrema is negligible in determining the excitation energy, as the distances between the extrema ΔU_B already exhibit significant fluctuations.

The distances ΔU_B between the extrema are now calculated, always measuring the distance between either two minima or two maxima. The individual distances are then indexed as described

in Equation 3. Here, the distance between the 1st and 2nd minima corresponds to an index of $n = 2$, and the distance between the 2nd and 3rd minima corresponds to an index of $n = 3$. The indices of the maxima are 0.5 values and are chosen in the same manner as the minima. The resulting data can be seen in Figure 7. It is observable that the distances between the extrema increase continuously. Therefore, a linear fit was applied to both the minima and maxima, as by definition the actual excitation energy can be determined at the point $n = 0.5$. It is visible that both linear fits converge to approximately the same value at $x = 0.5$, which is a good indication. However, the script [1] mentions that the first maximum is influenced by the characteristics of the tetrode. For this reason, we decided to disregard the linear fit of the maxima and only consider the linear fit of the minima ($\chi^2_{r,Min} = 1.25$). For this, the intersection at $x = 0.5$ is $S = (16.3(9)eV|0.5n)$. Thus, the excitation energy for neon gas is $E_a = 16{,}3(9)\,\mathrm{eV}$, which agrees with the literature value of $E_a = 16{,}6\,\mathrm{eV}$ [3].
With the determined value of E_a, the average free path length λ can now be calculated. Equation 4 is used for this purpose:

$$\lambda = \frac{L}{2E_a} \cdot m \tag{5}$$

Here, $L = 5\,\mathrm{mm}$ represents the distance between the two grids in the tetrode, and m denotes the slope of our linear fits from Figure 7. This yields a value of $\lambda = 0{,}31(5)\,\mathrm{mm}$.

Table 1: x-values of minima and maxima

	Orange	Blue	Green	Purple	Red
1. Min	2.5672(6)	2.6211(6)	2.6484(6)	2.7703(6)	2.8008(6)
2. Min	4.5727(4)	4.6086(4)	4.6063(4)	4.6227(4)	4.7195(4)
3. Min	6.6625(3)	6.6766(3)	6.7375(3)	6.8281(3)	6.8836(3)
1. Max	2.0008(3)	2.0008(3)	2.0008(3)	2.0000(3)	2.0008(3)
2. Max	3.8008(4)	3.8000(4)	3.8008(4)	3.8008(4)	3.8297(4)
3. Max	5.8140(3)	5.8000(3)	5.8117(3)	5.8297(3)	5.8375(3)

Table 2: Fitparameter for orange curve with form: $y = a \cdot (x - d)^2 + e$

	a	d	e	χ^2_r
1. Min	5.89(4)	2.5240(6)	-1.3051(13)	1.0009
2. Min	4.35(3)	4.5691(4)	0.3510(8)	1.0009
3. Min	2.472(12)	6.6469(3)	2.4875(3)	1.0009
1. Max	-6.65(3)	1.9844(3)	-0.5043(9)	1.0009
2. Max	-8.23(5)	3.8003(4)	1.777(2)	1.0009
3. Max	-4.34(2)	5.8175(3)	3.3099(6)	1.0008

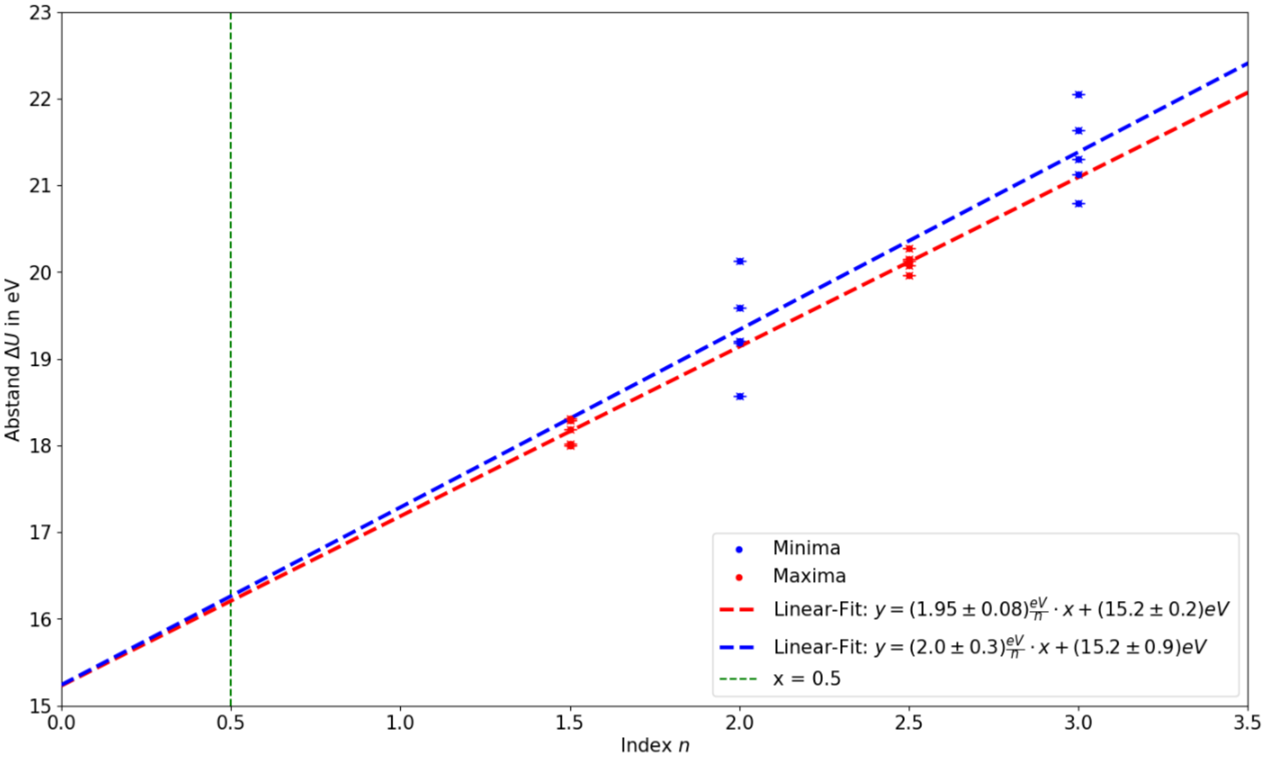

Figure 7: The figure plots the distance ΔU_B against the index n of the distance. The data for determined minima and maxima distances are depicted and differentiated by color (see legend). Additionally, the value for $n = 0.5$ is marked in green.

The last task involved removing the background from the data. For this purpose, a measurement was conducted with $U_1 = 7{,}5\,\mathrm{V}$ and $U_3 = 6{,}5\,\mathrm{V}$, depicted in Figure 8. Various functions were fitted to the data and subtracted. A 4th order polynomial provided the best fit with the lowest $\chi_r^2 = 1.0001$. After subtracting the function from the data, the dataset shown in Figure 9 was obtained, which is corrected for background. To verify this, a linear fit was applied, revealing no residual background slope within its error range.

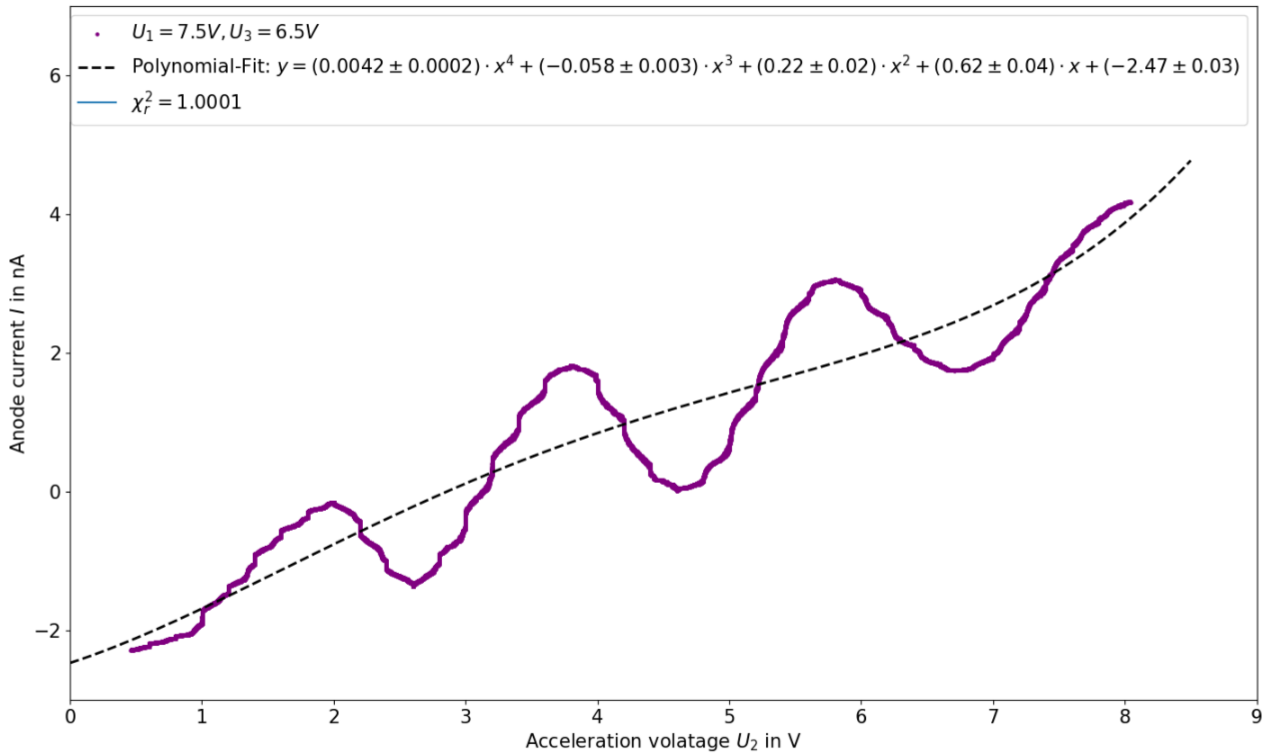

Figure 8: The figure plots the anode current I against the acceleration voltage U_2. The shown measurement was recorded at $U_1 = 7{,}5\,\mathrm{V}$ and $U_3 = 6{,}5\,\mathrm{V}$. A 4th order polynomial fit has been applied to the data, characterized by the form specified in the legend.

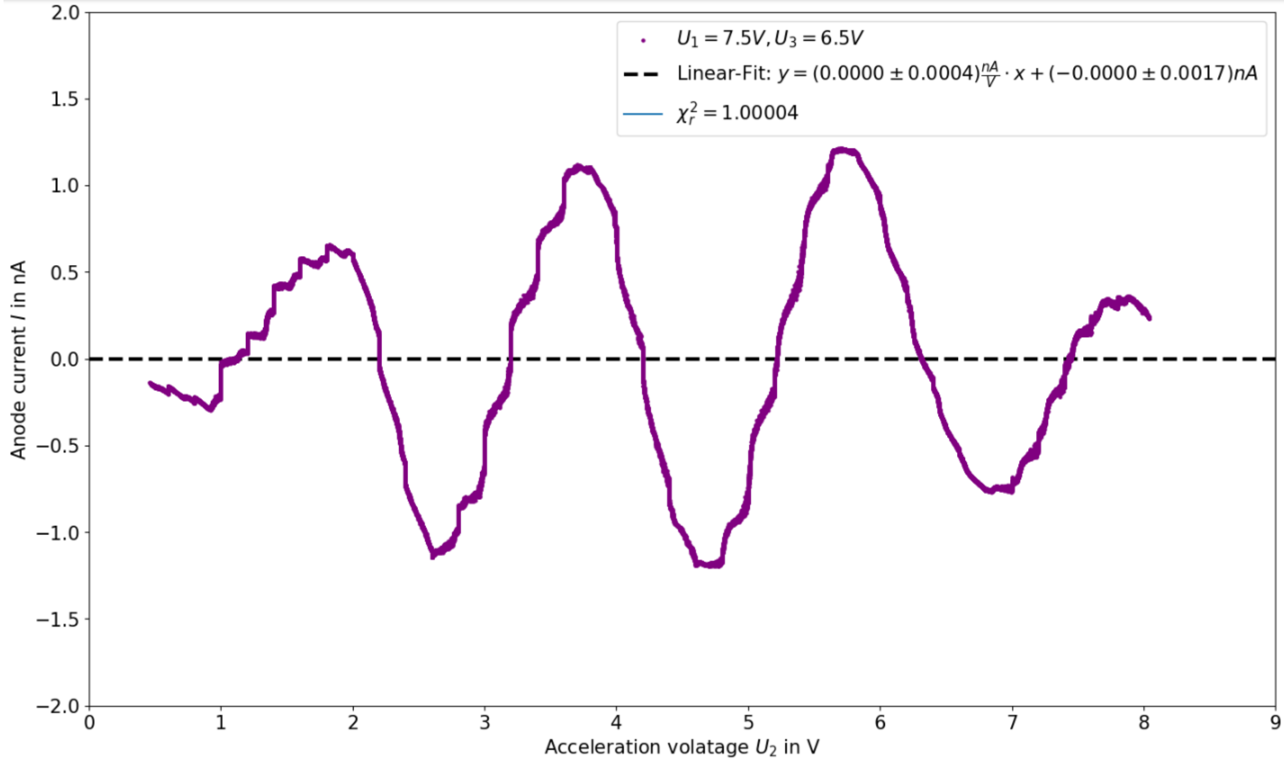

Figure 9: The figure displays the data from Figure 8 after background correction. A linear fit has been applied, as described by the form in the legend.

5 Discussion

The experiment proves to be very interesting as the energy levels of neon gas atoms can be clearly explained by the minima in relation to the theory of inelastic collisions, which in turn provides us with information about the characteristics of the atoms and their energy level structure. Additionally, it illustrates how the tetrode operates and the effects of varying the control grid voltage U_1 and the reverse bias voltage U_3 on the anode current. From our data, we were also able to determine the excitation energy of the first excited state $E_a = 16{,}3(9)\,\mathrm{eV}$ of neon gas by analyzing the distances between the minima. From this, we can also calculate the mean free path length as $\lambda = 0{,}31(5)\,\mathrm{mm}$. Furthermore, we were able to extract a clear background from our data.

References

[1] U. Innsbruck. *FP-Versuch E065: Franck-Hertz Stoßversuch*. Skript; retrieved on 18.06.24.

[2] 3. S. PHYSICS. *Betriebsgerät für Franck-Hertz-Experiment Betriebsanleitung*. Skript; retrieved on 18.06.24.

[3] NIST. *Energy Levels of Neutral Neon (Ne I)*. Skript; retrieved on 18.06.24. URL: https://pml.nist.gov/PhysRefData/Handbook/Tables/neontable5.htm.

Explanation

We hereby confirm that this report has been independently written and that all necessary sources and references have been cited.

Arik Bürkle	18.06.2024
Student 1	Date

Robin Hoffmann	18.06.2024
Student 2	Date

Valentin Ertl	18.06.2024
Student 3	Date

Workload

Arik Bürkle
Vorbereitung:4h
Versuch:2h
Bericht:3h
Robin Hoffmann
Vorbereitung:3h
Versuch:3h
Bericht:19h
Valentin Ertl
Vorbereitung:4h
Versuch:2h
Bericht:8h